



HAL
open science

Insights into the Headgroup and Chain Length Dependence of Surface Characteristics of Organic-Coated Sea Spray Aerosols

S. Cheng, S. Li, N. Tsona, C. George, L. Du

► **To cite this version:**

S. Cheng, S. Li, N. Tsona, C. George, L. Du. Insights into the Headgroup and Chain Length Dependence of Surface Characteristics of Organic-Coated Sea Spray Aerosols. *ACS Earth and Space Chemistry*, 2019, 3 (4), pp.571-580. 10.1021/acsearthspacechem.8b00212 . hal-02146490

HAL Id: hal-02146490

<https://hal.science/hal-02146490v1>

Submitted on 28 Nov 2019

HAL is a multi-disciplinary open access archive for the deposit and dissemination of scientific research documents, whether they are published or not. The documents may come from teaching and research institutions in France or abroad, or from public or private research centers.

L'archive ouverte pluridisciplinaire **HAL**, est destinée au dépôt et à la diffusion de documents scientifiques de niveau recherche, publiés ou non, émanant des établissements d'enseignement et de recherche français ou étrangers, des laboratoires publics ou privés.

Insights into the head-group and chain-length dependence of surface characteristics of organic-coated sea spray aerosols

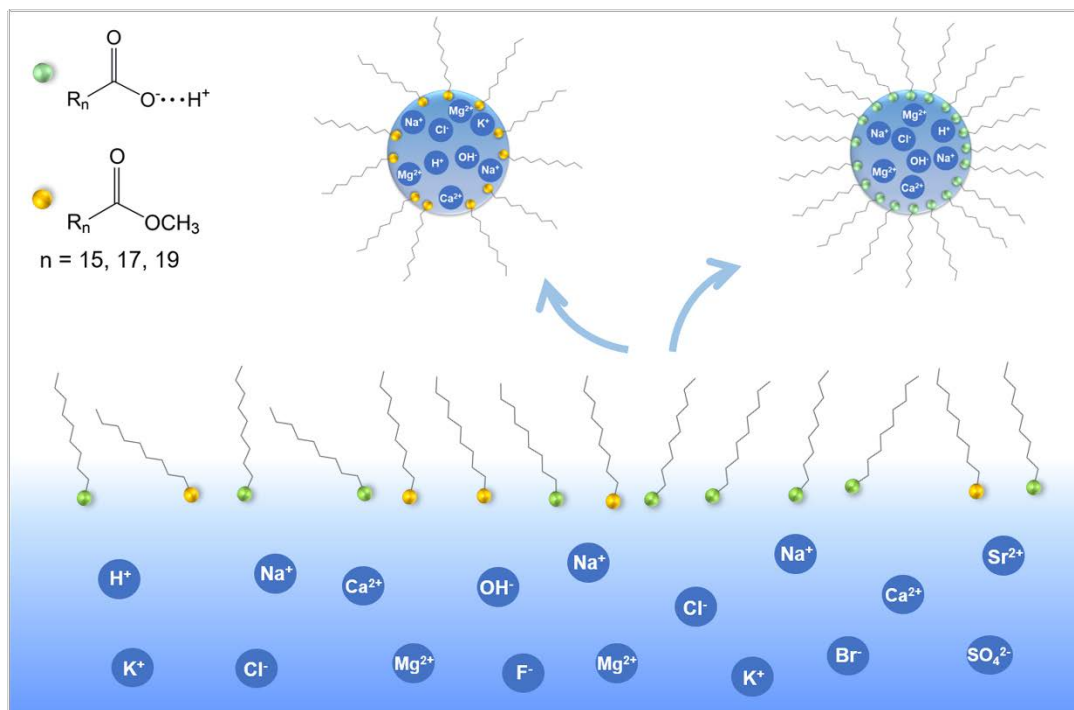
Shumin Cheng,[†] Siyang Li,[†] Narcisse T. Tsona,[†] Christian George,^{‡,§} and Lin Du^{*,†}

[†]Environment Research Institute, Shandong University, Binhai Road 72, Qingdao 266237, China

[‡]School of Environmental Science and Engineering, Shandong University, Binhai Road 72, Qingdao 266237, China

[§]University of Lyon, Université Claude Bernard Lyon 1, CNRS, IRCELYON, F-69626 Villeurbanne, France

Corresponding author: Email: lindu@sdu.edu.cn, Tel: +86-532-58631980



17 **ABSTRACT**

18 The structure of sea spray aerosols (SSAs) has been described as a saline core coated by organic
19 surfactants. The presence of surface-active compounds at the air-water interface can have a large
20 impact on physical, chemical and optical properties of SSAs. The surfactant molecules chosen for
21 this study, palmitic acid (PA), stearic acid (SA), arachidic acid (AA), methyl palmitate (MP), methyl
22 stearate (MS) and methyl arachidate (MA), were used to investigate the effect of alkyl chain-length,
23 head-groups and sea salts on the surface properties of these monolayers. A Langmuir trough was used
24 for measuring surface pressure–area (π -A) isotherms to reveal macroscopic phase behavior of the
25 surface films at the air-water interface. Infrared reflection absorption spectroscopy (IRRAS) was
26 employed to have a molecular-level understanding of the interfacial molecular organization. The π -A
27 isotherms indicated that sea salts, present in the subphase, exert a strong condensing effect on fatty
28 acid monolayers, while exerting expanding effect on fatty acid methyl ester monolayers, which was
29 confirmed by results from IRRAS experiments. IRRAS further revealed that the alkyl chains were in
30 an *all-trans* conformation, which can be evidenced by the relatively low $\nu_a(\text{CH}_2)$ and $\nu_s(\text{CH}_2)$
31 stretching frequencies. The conformational order changes in the alkyl chains of different film-forming
32 species ($\text{C16} < \text{C18} < \text{C20}$) were directly revealed by analyzing the relative intensity of the $\nu_a(\text{CH}_2)$
33 and $\nu_s(\text{CH}_2)$ peaks in the C-H stretching region. Thus, all the three factors alter the phase behavior
34 and molecular packing of the monolayers at the air-aqueous interface.

35

36 **Keywords:** Langmuir films; fatty acid; fatty acid methyl ester; sea spray aerosols; sea surface
37 microlayer

38

39 1. INTRODUCTION

40 Based on mass concentration, sea spray aerosol (SSA) is one of the largest sources of primary
41 atmospheric aerosol particles.¹⁻² SSAs formed at the sea surface microlayer through bubble-mediated
42 processes, are commonly composed of a sea salt core coated by a thin organic layer.³⁻⁶ This organic
43 layer is enriched with various organic species from both biological and anthropogenic sources, among
44 which, surface-active species account for a significant portion.^{5,7} Moreover, surface-active species in
45 the sea surface microlayer are expected to be more efficiently transferred into SSA, thus exhibiting
46 much higher concentration than that measured in the sea surface microlayer.⁷⁻⁹ Organic films present
47 in SSAs are reported to have inverse micelle structures with the hydrophilic head-groups toward the
48 aqueous phase and the hydrophobic tails to the air.¹⁰⁻¹¹ The morphology and conformation of organic
49 films will affect aerosol growth and volatility,¹² radiative absorption and scattering,^{6,13} reactivity with
50 atmospheric gases,¹⁰ and cloud condensation nuclei activity.^{3,8,14-15} Thus, understanding the surface
51 characteristics of surfactant molecules is important in atmospheric chemistry because of their
52 significant influence in physical, chemical and optical properties of SSAs.^{10,16}

53 Previous measurements suggested that fatty acids make up a large fraction of the organic
54 materials residing at the interface of marine aerosols.^{4,7,17} Fatty acids present in sea surface microlayer
55 are released primarily during the lysis of phospholipid cellular membranes of marine organisms.^{11,14}
56 Saturated fatty acids, particularly palmitic acid (PA) and stearic acid (SA), contribute significantly to
57 the organic coating of sea salt particles,^{11,18-19} with arachidic acid (AA) showing a relatively lower
58 abundance.²⁰ On the other hand, a former analysis of marine aerosols collected over the
59 Mediterranean Sea using a five-stage cascade impactor, found the existence of fatty acid methyl esters
60 from C14 to C34 in SSAs, among which, methyl palmitate (MP) and methyl stearate (MS) were found
61 to be predominant.²¹⁻²² Natural sources of these fatty acid methyl esters from hydrolysis of various
62 biosynthesized esters such as triglycerides, glycolipids, phospholipids, or waxes, have been
63 reported.²¹ Degradation of particulate material suspended in seawater from marine organisms has
64 been found to be the source of saturated and unsaturated fatty acid methyl esters.²³

65 Investigation of the surface properties of these organics at the air-water interface can provide a
66 better understanding of the chemical and physical processes taking place at the surfaces of SSAs in
67 the atmosphere. The film-forming species selected for this research are long chain fatty acids and
68 fatty acid methyl esters with alkyl chain-lengths of C16, C18 and C20. Langmuir trough has been
69 extensively used in atmospheric chemistry to understand the properties of surfaces and surfactant
70 molecules at the interface of aqueous aerosols.^{10,16} Surface pressure–area (π -A) isotherms of

71 Langmuir monolayers on aqueous surfaces are capable of revealing the underlying phase information
72 of the monolayers being subject to constant compression. However, to gain molecular-level insights
73 into the monolayers, spectroscopic techniques are needed. Infrared reflection absorption spectroscopy
74 (IRRAS) is a helpful technique in studying surface phenomena. Possessing the advantage of being a
75 fast and nondestructive technique,²⁴ IRRAS is sensitive to Langmuir monolayers if sufficient scans
76 are taken to obtain spectra with good signal-to-noise ratios.²⁵ The application of IRRAS enables us
77 to acquire information about molecular structure, conformation, and orientation of the film-forming
78 species.²⁵⁻²⁷ There are extensive studies elucidating the microscopic profile of Langmuir films of
79 saturated fatty acids at the air-water interface using IRRAS.^{4,28-30} In addition, fatty acid methyl esters
80 are also known to be able to form organized structures at the air-water interface.³¹⁻³⁴ Previous studies
81 of saturated long chain fatty acid and fatty acid methyl ester monolayers were carried out at the air-
82 water interface with IRRAS technique, by which the conformational order of the monolayers were
83 shown to be increased with increasing alkyl chain-length.³⁵⁻³⁶ The response of SA and AA Langmuir
84 monolayers to atmospheric inorganic ions was explored by Langmuir and IRRAS methods, which
85 confirmed the existence of inorganic ions in the fatty acid monolayers and its impact on the surface
86 properties of aqueous-phase aerosols.¹⁵ Former investigations were mainly conducted on pure water
87 (PW) or ion-containing subphases. However, properties of sea surface relevant surfactant monolayers
88 on the artificial seawater (ASW) subphase have been rarely studied.³⁷ The ASW used in this work is
89 pure water enriched with relevant sea salts, which is more representative of the environment that the
90 surfactant monolayers are exposed to.

91 In the present study, fatty acid/fatty acid methyl ester-ASW systems were chosen as proxies to
92 further understand the surface properties of marine aerosols. To investigate the influence of sea salts
93 on the studied monolayers, PW was also used as aqueous phase for comparison. Phase behavior and
94 molecular-level features of the fatty acid (PA, SA, AA) and fatty acid methyl ester (MP, MS, MA)
95 monolayers at the air-aqueous interface were examined using π -A isotherms and IRRAS spectra.
96 These compounds commonly have a carboxylic or methyl ester head-group connected to a saturated
97 hydrocarbon chain with different chain-lengths. The objective of the experiments outlined in this
98 paper is to determine the effect of alkyl chain-length, head-groups and sea salts on the properties of
99 the surfactant monolayers at the air-aqueous interface.

100

101 **2. EXPERIMENTAL SECTION**

102 **2.1 Materials.** PA ($\geq 98\%$, Adamas-beta), SA (98%, Aladdin), AA (99%, Aladdin), MP (99%,
103 Aladdin), MS (99%, Aladdin) and MA ($\geq 98\%$, Aladdin) were used without further purification. These
104 chemicals were dissolved in chloroform to a final concentration of 1 mM. Ultrapure water with a
105 resistivity of 18.2 M Ω was obtained from a Millipore Milli-Q purification system. ASW (see Table
106 1 for the detailed composition and concentrations) is a ten components mixture with a total
107 concentration of approximately 0.53 M.³⁷⁻³⁸ Specifically, it consists of: NaCl ($\geq 99\%$, Acros Organics),
108 Na₂SO₄ (99%, Alfa Aesar), KCl (3 M, Alfa Aesar), NaHCO₃ (≥ 99.7 , Alfa Aesar), KBr ($\geq 99\%$, Alfa
109 Aesar), H₃BO₃ (99.5%, Innochem), NaF ($\geq 99\%$, Acros Organics), MgCl₂·6H₂O (≥ 99 , Aladdin),
110 CaCl₂·2H₂O (99%, Adamas-beta), SrCl₂·6H₂O (≥ 99 , Alfa Aesar). All these salts were used as
111 received. The pH of the ASW was measured in the range of 8.0 ± 0.2 , a value representative of the
112 real seawater. The prepared ASW solution was allowed to equilibrate for several hours before
113 experiments were conducted.

114

115 **Table 1.** Composition of the artificial seawater

Type of cation	Salt	Concentration in aqueous solution (mM)
monovalent	NaCl	426
	Na ₂ SO ₄	29.4
	KCl	9.45
	NaHCO ₃	2.43
	KBr	0.857
	H ₃ BO ₃	0.438
	NaF	0.0744
divalent	MgCl ₂ ·6H ₂ O	55.5
	CaCl ₂ ·2H ₂ O	10.8
	SrCl ₂ ·6H ₂ O	0.0937

116

117 **2.2 Monolayer Spreading and Isotherm Measurements.**

118 The surface pressure π is a measurement of the difference between the surface tension when the
119 surface is covered in a surfactant and the surface tension of the bare surface ($\pi = \gamma_0 - \gamma_{\text{Langmuir}}$, where
120 γ_0 is the surface tension of pure water and γ_{Langmuir} is the surface tension of water with the Langmuir
121 film at the air-water interface).^{16,39} The surface tension value of ASW was calculated to be in the
122 range of 73.7-74.0 mN/m at 291 ± 1 K (details are given in the Supporting Information). Standard
123 deviations of the molecular area and surface pressure were $\pm 1 \text{ \AA}^2/\text{molecule}$ and $\pm 0.5 \text{ mN/m}$,
124 respectively.

125 π -A isotherms of the monolayers at the air-aqueous interface were recorded using a computer-
126 controlled Langmuir trough with two movable barriers sitting on top of the aqueous surface. The
127 trough is made out of Teflon and has inside dimensions of 65 mm \times 280 mm \times 3 mm. It was placed
128 on a vibration isolation table and closed in a Plexiglas box. At the beginning of the experiments, the
129 two barriers were placed at the ends of the trough. Tens of microliters of chloroform solutions of fatty
130 acids or fatty acid methyl esters were spread dropwise onto PW or ASW subphase using a glass
131 microsyringe. After deposition, about 15 min was allowed before compression to permit the solvent
132 to evaporate and the film to spread spontaneously. A pressure sensor with a Wilhelmy plate made
133 from a piece of rectangular filter paper was used to monitor the surface pressure with high sensitivity.
134 The π -A isotherms were obtained with the pressure sensor while the surface area available for the
135 surfactant molecules was decreased between the barriers. The monolayer at the air-aqueous interface
136 was continuously compressed at a constant rate of 3 mm/min. All experiments were performed at
137 ambient temperature (291 ± 1 K). Each experiment was run at least three times to ensure
138 reproducibility.

139

140 **2.3 IRRAS Measurements.** IRRAS spectra of the monolayers were recorded on a Bruker Vertex 70
141 FTIR spectrometer equipped with an external variable angle reflectance accessory for monolayer
142 measurements. To have maximum signal strength, the incidence angle of the IR beam was set at 40°
143 with respect to the surface normal. IRRAS spectra were collected over the range of 4000-400 cm^{-1} by
144 using a liquid-nitrogen cooled HgCdTe (MCT) detector and averaged for 2000 scans at a resolution
145 of 8 cm^{-1} . For IRRAS spectra collection, the monolayers were continuously compressed to a desired
146 surface pressure from ~ 0 mN/m. When the barriers were stopped, IRRAS spectra were obtained after
147 a time delay of 60 s, allowed for film equilibrium between trough movement and data collection.
148 IRRAS spectra were obtained at the surface pressure of 28 mN/m, which corresponded to the untilted
149 condensed phase of the π -A isotherms. During the IRRAS data collection, surface pressure changed
150 slightly for the monolayers (≤ 0.2 mN/m).

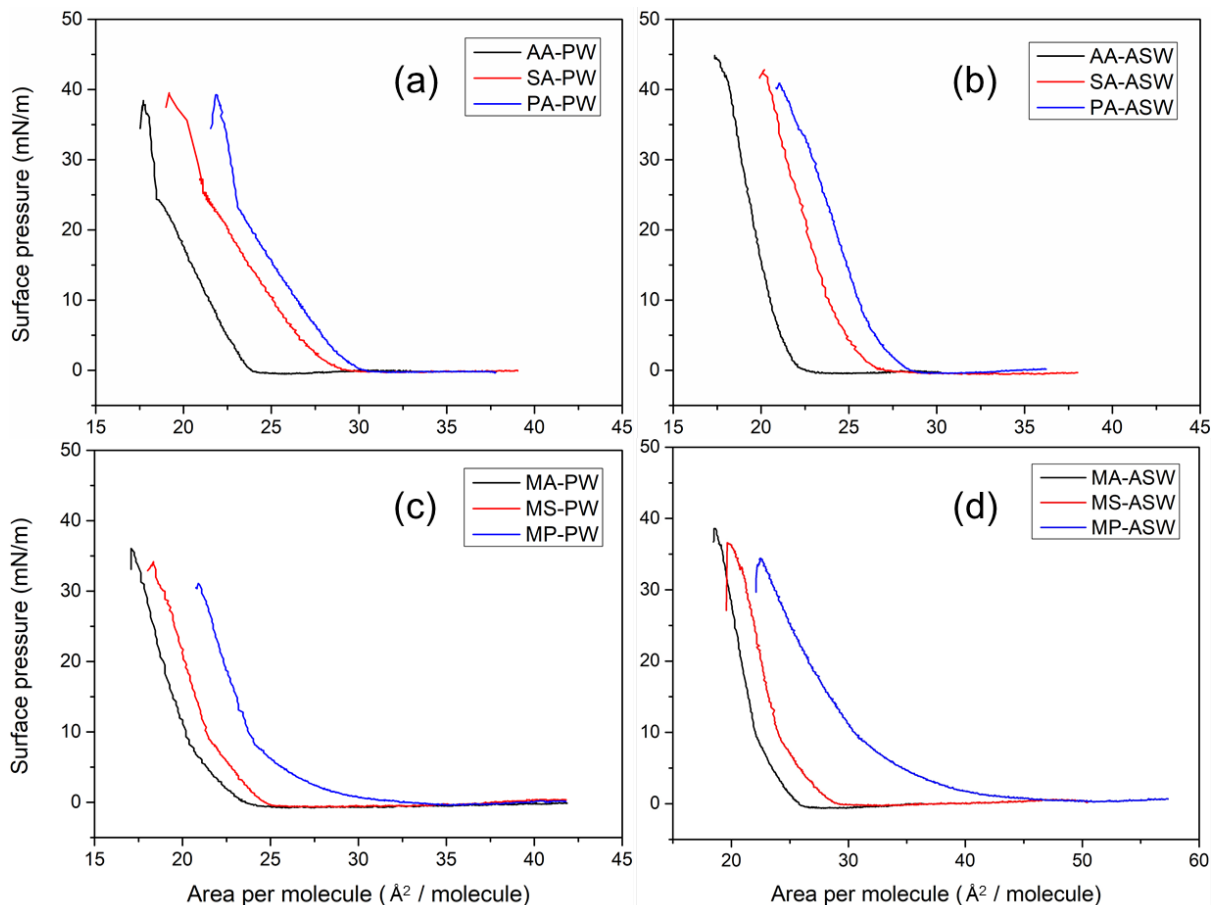
151

152 **3. RESULTS AND DISCUSSION**

153 **3.1 Surface Pressure–Area Isotherm.** π -A isotherms provide information about the phase behavior
154 of the monolayers at air-water interfaces. During the movement of the barriers, the phase of the
155 surface monolayer changes with the increase of the surface pressure. The phase changes can thus be
156 recognized from characteristics of the π -A isotherms. The surface pressure monitored as a function

157 of surface area of fatty acid and fatty acid methyl ester monolayers at room temperature are shown in
158 Figure 1. These π -A isotherms show remarkable changes along with alkyl chain-length, head-groups,
159 and aqueous subphases.

160



161

162 **Figure 1.** Surface pressure–area isotherms of fatty acid ((a), (b)) and fatty acid methyl ester ((c), (d))
163 monolayers on pure water (PW) and artificial sea water (ASW) subphases.

164

165 It can be seen from Figure 1(a) that the monolayers of fatty acids on pure water (PW) subphase
166 exhibit the following typical features in π -A isotherms upon compression. At low surface pressure
167 ($\pi = 0$ mN/m), the fatty acid monolayers show a gaseous-tilted condensed (G-TC) coexistence phase
168 before the lift-off area. In this phase, the alkyl chains are mostly free in space.⁴⁰ And then, the
169 monolayers were enforced into a tilted condensed (TC) phase after subsequent compression. In this
170 phase, there are less spatial movements for the fatty acid molecules. Further compression results in a
171 kink indicates a second-order phase transition from TC to an untilted condensed (UC) phase. In the
172 UC phase the hydrocarbon chains of fatty acids are almost perpendicular to the water subphase.¹⁶ In

173 addition, the surface pressure of second-order phase transitions from TC to UC phase upon
174 compression occur at about 24 mN/m, which is consistent with previous studies.^{25,41-42} Finally,
175 compressing the monolayer even further leads to a collapse state where the monolayer forms three-
176 dimensional structures because the surface is no longer stable.^{16,43-44}

177 The π -A isotherms of fatty acids obtained on ASW subphase are presented in Figure 1(b). The
178 isotherm conducted solely with the ASW subphase is shown in Figure S1, from which can be seen
179 that the surface pressure fluctuates around 0 mN/m, indicating that no or negligible surface active
180 substance is present in the ASW subphase. Thus, the influence of organic contaminants present in sea
181 salts can be ruled out. In the presence of sea salts, some changes are found in comparison with the
182 isotherms obtained on the PW subphase. It can be clearly seen that the TC phase disappears, as well
183 as the second-order phase transition. Beyond the lift-off points, the surface pressure increases steeply
184 with a formation of UC phase until the collapse of the monolayers occurs. This is in agreement with
185 a previous report studying the π -A isotherms for PA monolayers formed on CaCl₂ solution in.²⁵ This
186 behavior was attributed to the condensing effect of metal cations as a result of forming fatty acid
187 salts.^{25,45} Thus, a more orderly packed structure can be speculated for fatty acid monolayers on ASW
188 subphase. The differences in properties of π -A isotherms between Figures 1(a) and 1(b) indicate that
189 sea salts present in the subphase alter the macroscopic phase behavior of the long chain fatty acid
190 monolayers.

191 A strong chain-length dependence of fatty acids is also observed, as the lift-off areas are
192 concerned, which becomes gradually smaller with increasing chain-length. The lift-off areas of the
193 isotherms on PW are 30.3, 29.3 and 24.2 Å²/molecule for PA, SA and AA, respectively. The sequence
194 and general shape of the interfacial isotherms herein are consistent with previous reports.^{37,46-47} The
195 chain-length dependence of lift-off areas indicates that the van der Waals energy increases with the
196 length of chain, and draws the molecules closer as the intermolecular attraction increases.⁴⁷⁻⁴⁸ On the
197 other hand, compared to PW, condensation of the fatty acid monolayers occurs when ASW is used
198 as subphase as illustrated in Figure 1(b). It is evident that with ASW as subphase, the lift-off areas
199 are decreased for individual fatty acids. The change in lift-off areas for PA, SA and AA are -1.4, -2.2,
200 -1.7 Å²/molecule, respectively. Consequently, all the studied fatty acid molecules become more
201 densely packed on ASW than on PW.⁴⁶ At the air-ASW interface, the favorable electrostatic
202 interaction or complexation between fatty acids and sea salts leads to a denser chain packing relative
203 to that of air-PW interface.⁴⁹

204 Being molecules with saturated single alkyl chains like fatty acids, fatty acid methyl ester

205 molecules are fairly compressible as well, and ultimately, can be packed in a highly ordered structure
206 at high surface pressures. As can be seen from Figures 1(c) and 1(d), the slight TC-UC transition
207 occurs at about 8 mN/m as the surface pressure rises for all the three fatty acid methyl ester
208 monolayers, irrespective of the subphase. Specifically, the π -A isotherm obtained for MP in this
209 study is consistent with a previous research about the temperature dependence of MP monolayers,
210 which found that they are fully condensed below 293 K and no plateau can be observed in the
211 isotherm.^{35,50} Unlike fatty acid monolayers, the presence of sea salts does not change significantly the
212 shape of fatty acid methyl ester isotherms, although a clear shift to larger mean molecular areas can
213 be observed. Thus, sea salts exert an opposite effect on fatty acid methyl esters compared to fatty
214 acids, resulting in an expansion of the fatty acid methyl ester monolayers. The lift-off areas are clearly
215 observed at about 34.6 and 25.4 and 24.4 Å²/molecule for MP, MS and MA monolayers on PW,
216 respectively. However, when ASW is used as subphase, the values shift to about 45.5, 29.3 and 26.3
217 Å²/molecule. Similarly, a former investigation of MP on PW and NaCl solutions with different ion
218 concentrations (1, 2 and 3 M), found the expanding effect of NaCl on the MP monolayer from the
219 increasing lift-off area with increasing NaCl concentration.⁵⁰ The reason of this behavior was
220 explained to be the increased ionic strength, which influences interactions of the water molecules
221 with the carboxyl group.

222 To sum up, the presence of sea salts in the subphase has opposite effects on the fatty acid and
223 fatty acid methyl ester monolayers. In addition, similar with fatty acids, the π -A isotherms of fatty
224 acid methyl esters shift to smaller molecular areas with increasing chain-length. Hence, further
225 increase in the hydrocarbon chain-length results in more densely packing of the fatty acid methyl
226 ester molecules. Thus, the conformational order of the alkyl chains increases with increasing chain-
227 length can be concluded from the π -A isotherms: C16 < C18 < C20, irrespective of head-groups or
228 subphases.

229 When comparing Figures 1(b) and 1(d), the difference in π -A isotherms on ASW subphase
230 indicates that the phase sequence is changed because of the esterification of the carboxyl group, with
231 the appearance of TC phase and second-order phase transitions in fatty acid methyl ester monolayers.
232 When ASW is used as subphase, it can be seen from Figures 1(b) and 1(d) that the lift-off areas of
233 fatty acid methyl esters are much larger than corresponding fatty acids. The main difference between
234 the fatty acids and the fatty acid methyl esters is the head-group structure, where the acids are
235 sensitively influenced by the subphase pH. Empirical evidence suggests that under the conditions of
236 about pH=8.2, the carboxyl group is partially dissociated to be negatively charged.^{4,25,51} It is likely

237 that the stability and surface activity of these long chain fatty acids decrease upon dissociation of the
238 carboxylic acid proton.⁴ However, the stability of these monolayers can be greatly improved by
239 electrostatic attractions or complexation with various sea salts in the aqueous subphase.^{49,52} By means
240 of IRRAS, the surface propensity of PA molecules was found to be increased by adding NaCl into
241 the subphase,⁴ suggesting that deprotonated fatty acids may be found at the air-aqueous interface due
242 to the role of sea salts in surface stabilization. A study of SA monolayers was carried out on 1, 10 and
243 100 times diluted ASW.³⁷ The π -A isotherms of the SA monolayers show an enhanced stability of
244 the film against fracture when the sea salt concentration of the subphase was higher. In case of fatty
245 acid methyl esters, no effect is expected due to ionization of head-groups, because the pH of the
246 subphase is too low to observe any measurable hydrolysis of the esters. The observed different trends
247 in the isotherms may in part be due to the different interaction mechanisms between the sea salts and
248 the head-groups.

249 It has been well documented that at low surface pressure, the methyl ester head-group is *E*-
250 configured for expanded fatty acid methyl ester monolayers, where substantial part of the oxo-methyl
251 group is pointing out of the water (Figure S2). The *E* isomer of fatty acid methyl esters allows the
252 hydration of the polar group and hinders the electrostatic interactions between hydrophilic head-group
253 and cation. However, at higher surface pressure, the head-group is *Z*-configured with the oxo-methyl
254 component directed into the water for more orderly packed compressed states.^{35,53} In addition, several
255 studies have described the expulsion of water molecules from the monolayer as surface pressure
256 increases.^{32-33,35} When the fatty acid methyl ester monolayers are in *Z*-configuration, the carbonyl
257 group is shielded by the oxo-methyl component and, thus, the carbonyl group is more or less
258 prevented from being hydrogen-bridged by water molecules. The expelled water from fatty acid
259 methyl ester films could affect the arrangement of *Z* isomer, allowing the cations to penetrate into the
260 film (Figure S3). In this way, the growth of three-dimensional structures could be favored because
261 the partial charge of the head-group of fatty acid methyl ester would be compensated.³³ Therefore,
262 we can speculate that the main cause of the instability of the fatty acid methyl ester monolayers in the
263 presence of sea salts is a collapse process which involves the formation of three-dimensional nuclei
264 on the monolayer surface.

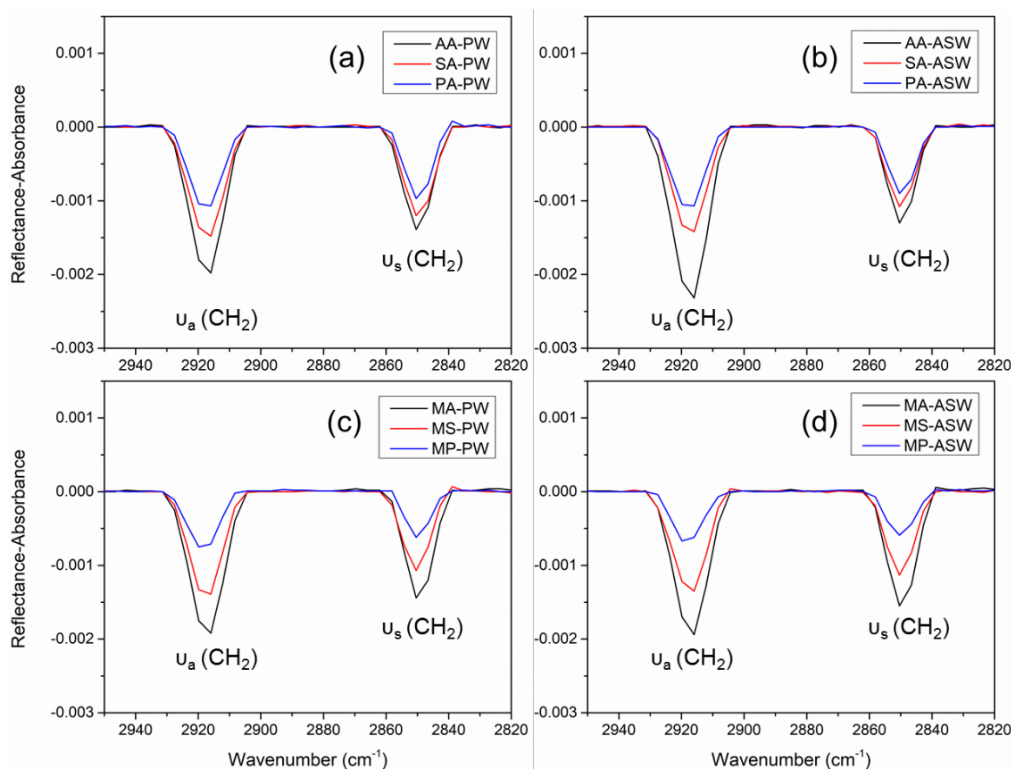
265 The above descriptions suggest that both interactions between adjacent amphiphiles and
266 interactions between amphiphiles and the subphase are important to the macroscopic phase behavior
267 of the monolayers. However, to get deep insights into microscopic molecular arrangement and
268 underlying mechanisms, advanced spectroscopic techniques are necessary. This consideration led us

269 to explore the molecular conformation of the monolayer films by means of the IRRAS technique.

270

271 **3.2 IRRAS Spectra.** The monolayers of fatty acids with different chain-lengths (PA, SA, and AA)
272 and corresponding fatty acid methyl esters (MP, MS, MA) on air-aqueous interface were examined
273 using IRRAS. This technique enables us to probe microscopic information such as the conformation
274 order and orientation of the monolayers at the molecular-level. The vibrational modes investigated
275 encompass both head and tail groups of the sample molecules. The stretching vibrations of C-H
276 ($\nu(\text{CH}_2)$) at 2820-2950 cm^{-1} , the $\nu(\text{COO})$ and scissoring band of C-H ($\delta(\text{CH}_2)$) at 1400-1500 cm^{-1} ,
277 and the $\nu(\text{C}=\text{O})$ at 1700-1800 cm^{-1} were probed.

278



279

280 **Figure 2.** IRRAS spectra (2820-2950 cm^{-1}) of the fatty acid ((a), (b)) and fatty acid methyl ester ((c),
281 (d)) monolayers recorded at 28 mN/m on pure water (PW) and artificial sea water (ASW) subphases
282 at the incidence angle of 40°.

283

284 IRRAS spectra (2820-2950 cm^{-1}) of the fatty acid and fatty acid methyl ester monolayers in the
285 UC phase on PW and ASW subphases are shown in Figures 2(a)-(d). In Figure 2(a), for fatty acid
286 monolayers on air-PW interface, the two bands at around 2916 cm^{-1} and 2850 cm^{-1} can be assigned
287 to the methylene antisymmetric ($\nu_a(\text{CH}_2)$) and methylene symmetric ($\nu_s(\text{CH}_2)$) stretching vibrations

288 of the hydrocarbon chains, respectively. At the incidence angle of 40° , these bands show negative
289 reflection absorbance. The $\nu_a(\text{CH}_2)$ and $\nu_s(\text{CH}_2)$ frequencies have been known to be sensitive to the
290 conformation order of hydrocarbon chains.^{45,54} Lower frequencies are characteristic of preferential
291 *all-trans* conformers in highly ordered chains, while the number of *gauche* conformers increases with
292 increasing frequency and width of the bands.^{17,29} For *all-trans* conformations of the fully extended
293 tail chains, the symmetric and asymmetric stretching vibrations of the methylene groups are usually
294 present in the narrow ranges of 2846-2850 and 2915-2918 cm^{-1} , respectively, and in the distinctly
295 different ranges of 2854-2856 and 2924-2928 cm^{-1} for disordered chains characterized by a significant
296 presence of *gauche* conformations.⁵⁵ The relatively low frequency positions of the $\nu_s(\text{CH}_2)$ and
297 $\nu_a(\text{CH}_2)$ stretching modes at about 2850 cm^{-1} and 2916 cm^{-1} , indicate that the alkyl chains are mostly
298 in highly ordered *all-trans* conformations.⁵⁶ This shows clearly that the alkyl chains are almost
299 perpendicular to the air-water interface. The *all-trans* conformation can also be found in other
300 compressed monolayers shown in Figures 2(b), 2(c) and 2(d), irrespective of the head-groups or the
301 subphases. The highly ordered structure of fatty acids directly correlates with the van der Waals
302 interaction between adjacent alkyl chains, the interactions between adjacent COOH head-groups and
303 those between head-groups and aqueous subphase. An orderly packed structure can maximize
304 interactions with an *all-trans* conformation between adjacent alkyl chains.²⁵ For the fatty acid methyl
305 ester monolayers, the steric demand in the *E*-configuration is very high. This structure results in quite
306 strongly tilted molecules and a poor conformational order. When the monolayer is further compressed,
307 a reduction of the available area forces molecules to approach each other and pack more densely. As
308 a compromise, the methyl group is squeezed into the subphase, thus resulting in a *Z*-conformation of
309 amphiphiles in the condensed phase. With this conformation, the oxo-methyl group facilitates the *all-*
310 *trans* configuration of the alkyl chains. Consequently, the head-group can be forced into the *Z*-
311 configuration with increasing surface pressure and result in the *all-trans* conformation of the alkyl
312 chains.³⁵

313 All the fatty acids and corresponding methyl esters commonly possess saturated hydrocarbon
314 chains with different chain-lengths. IRRAS bands arising from these alkyl chains provide the clear
315 spectra and hence reliable information about molecular conformation in the monolayers.³⁰ The peak
316 heights and areas of the $\nu_a(\text{CH}_2)$ and $\nu_s(\text{CH}_2)$ bands indicate the packing density of the alkyl chains.³⁵
317 It can be evidenced from Figure 2 that the peak heights and areas for the methylene stretching
318 vibrations increase with increasing chain-length, irrespective of head-groups or subphases. As the
319 directions of $\nu_a(\text{CH}_2)$ and $\nu_s(\text{CH}_2)$ vibrational modes are orthogonal to the molecular axis, strong

320 intensities of the bands indicate that the molecule stands nearly perpendicular to the water subphase
 321 when the hydrocarbon chain is in the *all-trans* conformation.⁵⁷ Hence, the much smaller peak
 322 intensity of C16 relative to the higher homologues is indicative of a substantially stronger tilt and less
 323 ordered conformation of the molecules, reflecting more orderly packed structure of higher
 324 homologues at the UC state. It is necessary to consider these data in relation to the π -A isotherms of
 325 Figure 1, which shows that smaller areas were occupied by monolayers formed by surfactants with
 326 longer alkyl chain-length.

327 **Table 2.** The peak-height intensity ratio between the antisymmetric and symmetric bands of the CH₂
 328 groups (I_{as}/I_s) for the fatty acid and fatty acid methyl ester monolayers on pure water (PW) and
 329 artificial sea water (ASW) subphases.

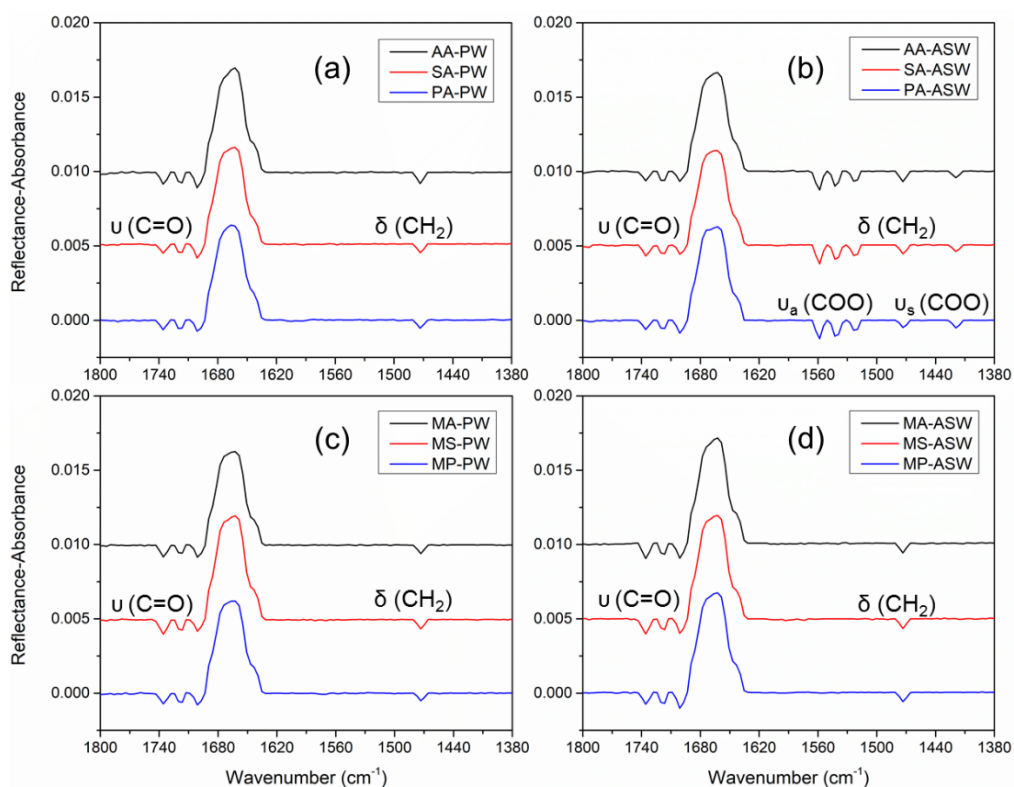
subphase	PA	SA	AA	MP	MS	MA
PW	1.10	1.23	1.43	1.21	1.29	1.33
ASW	1.19	1.32	1.78	1.14	1.19	1.26

331
 332 The conformational order changes in the alkyl chains introduced by sea salts, head-groups or
 333 alkyl chain-length can be further revealed by analyzing the relative intensity of the $\nu_a(\text{CH}_2)$ and the
 334 $\nu_s(\text{CH}_2)$ peaks in the C-H stretching region.¹⁵ The peak-height intensity ratios between the
 335 antisymmetric and symmetric bands of the CH₂ groups (I_{as}/I_s) for the studied monolayers are
 336 presented in Table 2 for direct comparison. In Figure 2, the intensities of $\nu_s(\text{CH}_2)$ peaks are relatively
 337 weaker than those of the $\nu_a(\text{CH}_2)$ peaks, thus giving I_{as}/I_s values greater than one. Qualitatively
 338 speaking, larger I_{as}/I_s ratio indicates more orderly packed alkyl chains with nearly *all-trans*
 339 conformation.⁵⁸⁻⁶⁰ It can be seen from Table 2 that the ratio values are smaller for monolayers formed
 340 by molecules with shorter alkyl chain-length, irrespective of head-groups or subphases, indicating the
 341 existence of *gauche* defects in corresponding monolayers. Therefore, the pronounced chain order
 342 increase with increasing chain-length can be concluded from IRRAS spectra: C16 < C18 < C20,
 343 which is in line with the conclusion obtained from the π -A isotherms (Figure 1). As was shown in
 344 the π -A isotherms, sea salts demonstrate a condensing effect on the fatty acid monolayers, which
 345 consequently leads to the absence of the TC phase. The IRRAS spectra obtained on the ASW surface
 346 confirm this effect, as can be seen from the larger intensity ratios of the $\nu_a(\text{CH}_2)$ over the $\nu_s(\text{CH}_2)$ than
 347 those on the PW subphase in individual spectra, with values of I_{as}/I_s increasing from 1.10, 1.23 and
 348 1.43 to 1.19, 1.32 and 1.78, respectively. This result can be attributed to the decrease in the

349 concentration of *gauche* defects and tilt angle of monolayers formed on ASW subphase. With respect
 350 to fatty acid methyl esters, the intensity ratios of I_{as}/I_s obtained on ASW (1.14, 1.19 and 1.26) surface
 351 are smaller than those on PW (1.21, 1.29 and 1.33), which indicates that the fatty acid methyl ester
 352 monolayers are disordered by sea salts. This can be evidenced by the expanding effect introduced by
 353 sea salts on fatty acid methyl ester monolayers. Therefore, IRRAS experiments confirm the contrary
 354 effects of sea salts on fatty acid and fatty acid methyl ester monolayers as can be observed from π -A
 355 isotherms.

356 Evidences of monolayer orientation and structural changes along with alkyl chain-length, head-
 357 groups, and subphases are provided mainly by details of the $\nu_a(\text{CH}_2)$ and the $\nu_s(\text{CH}_2)$ bands. Peak
 358 position, height, area and intensity ratios were utilized to support the analysis. These characteristics
 359 correlate well with those shown by the π -A isotherms. Information about the dependence of the chain
 360 order on the alkyl chain-length and subphases, i.e., the overall effect of an increase in alkyl chain-
 361 length leading to an increase in order, ASW acts to condense fatty acid films and expand fatty acid
 362 methyl ester films, was inferred from both the IRRAS spectra and the π -A isotherms. The IRRAS
 363 technique not only allows for the characterization of all the above chain conformation and orientation
 364 details, but also provides valuable information about molecular interaction between the monolayers
 365 and the aqueous subphase.

366



367

368 **Figure 3.** IRRAS spectra (1380-1800 cm^{-1}) of the fatty acid ((a), (b)) and fatty acid methyl ester ((c),
369 (d)) monolayers recorded at 28 mN/m on pure water (PW) and artificial sea water (ASW) at the
370 incidence angle of 40° .

371

372 Figure 3 shows IRRAS spectra (1800-1380 cm^{-1}) of the $\nu(\text{C}=\text{O})$, $\delta(\text{CH}_2)$ and $\nu(\text{COO})$ regions of
373 the fatty acid and fatty acid methyl ester monolayers in the UC phase on the PW and ASW subphases.
374 Three peaks are observed at 1739, 1720, and 1704 cm^{-1} , which can be attributed to the stretching
375 vibrations of the free C=O group, the C=O group involved in one and two hydrogen bonds,
376 respectively. A previous IRRAS investigation of SA monolayer at the air-water interface gave similar
377 results.³⁶ The ability of the carbonyl group to form hydrogen bonds was explained to be a mixture
378 effect of hydration by the water subphase and by side-bridging hydrogen-bond formation between
379 adjacent fatty acid molecules.^{36,61} The sharp singlet observed at 1472 cm^{-1} is ascribed to the $\delta(\text{CH}_2)$
380 band of the methylene groups.^{29,54}

381 IRRAS spectra of fatty acids on the ASW subphase (Figure 3 (b)) in the region of COO
382 stretching vibrations can provide insights into interaction mechanisms between carboxylic acid head-
383 groups and the subphase. In the presence of sea salts, additional peaks arising from the asymmetric
384 ($\nu_a(\text{COO})$) and symmetric ($\nu_s(\text{COO})$) stretching modes of the COO group are observed. The three
385 peaks including 1558, 1542, 1523 cm^{-1} are resulted from the splitting of the $\nu_a(\text{COO})$ stretching
386 vibration,¹⁵ while the peak at 1419 cm^{-1} is assigned to the $\nu_s(\text{COO})$ stretching mode.³⁸ Complexation
387 of ions to surface-active species has been known to alter their orientation, packing, and surface
388 morphology.^{17,62} The stability of the SA monolayer was found to be increased significantly at high
389 pH values due to ionization of the surfactant by Ca^{2+} and Mg^{2+} in the subphase.⁶³ It has been reported
390 that metal cations can bind to the carboxylate group in several ways including ionic binding,
391 unidentate type, bidentate chelate type and bidentate bridging type.²⁴ The bonding type of metal
392 cations to the carboxylate group in the UC state can be classified by the difference between the
393 antisymmetric and symmetric COO stretching frequencies. In this work, the differences in $\nu_a(\text{COO})$
394 and $\nu_s(\text{COO})$ stretching frequencies give three values of about 139, 123 and 104 cm^{-1} , respectively.
395 The difference in $\nu_a(\text{COO})$ and $\nu_s(\text{COO})$ stretching frequencies for dissociated acid was estimated to
396 be 138 cm^{-1} .²⁴ Typically, the values for bidentate bridging coordination are somewhat close to that
397 for a dissociated carboxylate ion, and values of bidentate chelate coordination are less than that of a
398 dissociated carboxylate ion.²⁴ Thus, the main component at 1558 cm^{-1} belongs to a bidentate bridging

399 structure, while the components at 1542 cm^{-1} and 1523 cm^{-1} can be attributed to bidentate chelate
400 coordinations. Hence, in the presence of the ASW subphase, dissociated fatty acids form bidentate
401 bridged and bidentate chelate coordinations. As the ASW used herein is a complex mixture of sea
402 salts, it is hard to distinguish which cation the fatty acids are binding to. In this regard, sea salts are
403 treated as a whole to consider their interaction with the head-groups of fatty acid and fatty acid methyl
404 ester molecules.

405

406 **3.3 Atmospheric Implications.** The organic films that reside at the air-water interface exert a
407 significant impact on many properties of SSAs, such as its ability to exchange species including water
408 molecules and traces gases across the interface,⁶⁴ its ability to absorb or scatter radiation,^{6,10,13} and its
409 reactivity towards oxidative gases.⁶⁵ Long chain fatty acid and fatty acid methyl ester monolayers at
410 the air-aqueous interface were utilized as simplified model of organic-coated SSAs. The impact of
411 sea salts, head-groups and alkyl chain-length on phase behavior and molecular organization of the
412 monolayer films was fully characterized. The higher stability of monolayers formed by species with
413 longer alkyl chain-length is clear. The lifetime of the hydrophobic layer on SSA is dependent on many
414 variables, an important one being the carbon chain-length of the surfactants comprising the coating.⁶⁵⁻
415 ⁶⁶ Properties of the aqueous core, including pH and composition, also affect the stability of the organic
416 surface films. Adding sea salts into the subphase improves the stability of the fatty acid films by
417 binding to the carboxylic acid groups through bidentate bridged and bidentate chelate coordinations.
418 Thus, deprotonated fatty acids may be found at the air-aqueous interface of aerosol particles partly
419 due to the role of sea salts in surface stabilization.

420 ASW caused condensation of the fatty acid surface films, leading to tightly packed molecules.
421 However, the expansion effect was introduced by ASW toward fatty acid methyl ester films, which
422 led to loosely packed molecules. Thus, we can speculate that fatty acid molecules reside at the
423 interface of SSAs with greater stability and higher packing density relative to fatty acid methyl esters.
424 This is in line with field measurements of marine aerosols utilizing time-of-flight secondary ion mass
425 spectrometry (TOF-SIMS) as a surface sensitive analysis technique. The aerosols collected in the
426 field exhibited surface layers dominated by fatty acids.⁶⁷ One major effect of surface active organic
427 monolayer shown both by observations and modeling, is the lowering of the particle surface
428 tension.^{39,68} Surface active species present at the air-water interface have the potential to lower the
429 surface tension of a growing droplet relative to pure water at a given relative humidity.⁶⁹ A lower
430 surface tension promotes small particle growth at lower relative humidity in accord with the Kelvin

431 effect⁶⁹⁻⁷⁰ and increasing particle cloud condensation nuclei activation efficiency,^{39,68} thereby causing
432 the droplets to grow larger than predicted. As can be seen from the surface pressure-area isotherms,
433 beyond the lift-off points, the surface pressure of the interface increases with decreasing mean
434 molecular areas, indicating the reduction of surface tension. The surface tension of ASW interface
435 covered by fatty acid reduces more rapidly along with decreasing mean molecular areas than in
436 corresponding methyl ester. Thus the effectiveness of the film on surface tension reduction will
437 depend on the species of film-forming molecules as well as chemical composition of the aqueous
438 core. In addition, the optical properties of aerosols are largely dependent upon their size and in this
439 regard, the alteration in aerosol size will affect their scattering efficiency.⁴⁶

440

441 **4. CONCLUSIONS**

442 In this work, monolayers of long chain fatty acids and fatty acid methyl esters (C16, C18, C20)
443 at the air-aqueous interface were used as proxies for the organic-coated SSAs. Both π -A isotherms
444 and IRRAS spectra were applied to systematically investigate the effect of alkyl chain-length, head-
445 groups and sea salts on the surface properties of organic monolayers. It was shown by π -A isotherms
446 that sea salts have a condensing effect on fatty acid monolayers, meanwhile, obvious differences in
447 phase behavior were detected over the PW and ASW subphases. However, an expansion effect of sea
448 salts on fatty acid methyl ester monolayers was observed, without any distinct change of the phase
449 transitions between π -A isotherms detected over the PW and ASW subphases. The pronounced chain
450 order increase with increasing chain-length (C16 < C18 < C20) was revealed by π -A isotherms,
451 irrespective of head-groups or subphases. These findings were further confirmed by IRRAS spectra.
452 Substantial intensity ratio increases in the I_{as}/I_s were observed on monolayers formed by species with
453 longer chain-length. From the differences between $\nu_a(\text{COO})$ and $\nu_s(\text{COO})$ stretching frequencies, the
454 dominant binding coordinations between deprotonated fatty acids and sea salts were found to be
455 bidentate bridging and bidentate chelate. These results indicate that the surface characteristics of
456 organic-coated SSAs are influenced by both the chemical composition of the aqueous core and
457 species of film-forming molecules.

458

459 **ASSOCIATED CONTENT**

460 **Supporting Information**

461 Calculation of surface tension of artificial seawater, surface pressure-area isotherms of artificial
462 seawater and isotherm of steric acid monolayer on artificial seawater subphase (Figure S1), schematic

463 representation of *E*- and *Z*-conformation of fatty acid methyl esters at the air-water interface (Figure
464 S2), and schematic representation of fatty acid methyl ester monolayers at the air-seawater interface
465 (Figure S3).

466

467 AUTHOR INFORMATION

468 Corresponding Author

469 *Email: lindu@sdu.edu.cn, Tel: +86-532-58631980

470 Notes

471 There are no conflicts of interest to declare.

472

473 ACKNOWLEDGMENTS

474 This work was supported by National Natural Science Foundation of China (91644214, 21876098),
475 Shandong Natural Science Fund for Distinguished Young Scholars (JQ201705) and the the Marie
476 Curie International Research Staff Exchange project MARSU (Grant 690958).

477

478 REFERENCE

- 479 (1) Braun, R. A.; Dadashazar, H.; MacDonald, A. B.; Aldhaif, A. M.; Maudlin, L. C.; Crosbie, E.;
480 Aghdam, M. A.; Mardi, A. H.; Sorooshian, A. Impact of wildfire emissions on chloride and bromide
481 depletion in marine aerosol particles. *Environ. Sci. Technol.* **2017**, *51* (16), 9013-9021.
- 482 (2) Quinn, P. K.; Coffman, D. J.; Johnson, J. E.; Upchurch, L. M.; Bates, T. S. Small fraction of
483 marine cloud condensation nuclei made up of sea spray aerosol. *Nat. Geosci.* **2017**, *10* (9), 674-679.
- 484 (3) Jayarathne, T.; Sultana, C. M.; Lee, C.; Malfatti, F.; Cox, J. L.; Pendergraft, M. A.; Moore, K. A.;
485 Azam, F.; Tivanski, A. V.; Cappa, C. D.; Bertram, T. H.; Grassian, V. H.; Prather, K. A.; Stone, E.
486 A. Enrichment of saccharides and divalent cations in sea spray aerosol during two phytoplankton
487 blooms. *Environ. Sci. Technol.* **2016**, *50* (21), 11511-11520.
- 488 (4) Adams, E. M.; Wellen, B. A.; Thiriaux, R.; Reddy, S. K.; Vidalis, A. S.; Paesani, F.; Allen, H. C.
489 Sodium-carboxylate contact ion pair formation induces stabilization of palmitic acid monolayers at
490 high pH. *Phys. Chem. Chem. Phys.* **2017**, *19* (16), 10481-10490.
- 491 (5) Tseng, R. S.; Viechnicki, J. T.; Skop, R. A.; Brown, J. W. Sea-to-air transfer of surface-active
492 organic-compounds by bursting bubbles. *J. Geophys. Res.: Oceans* **1992**, *97* (C4), 5201-5206.
- 493 (6) Tervahattu, H.; Hartonen, K.; Kerminen, V. M.; Kupiainen, K.; Aarnio, P.; Koskentalo, T.; Tuck,
494 A. F.; Vaida, V. New evidence of an organic layer on marine aerosols. *J. Geophys. Res.* **2002**, *107*
495 (D7-D8), AAC1-AAC9.
- 496 (7) Cochran, R. E.; Laskina, O.; Jayarathne, T.; Laskin, A.; Laskin, J.; Lin, P.; Sultana, C.; Lee, C.;
497 Moore, K. A.; Cappa, C. D. Analysis of organic anionic surfactants in fine and coarse fractions of
498 freshly emitted sea spray aerosol. *Environ. Sci. Technol.* **2016**, *50* (5), 2477-2486.
- 499 (8) Lin, W.; Clark, A. J.; Paesani, F. Effects of surface pressure on the properties of Langmuir
500 monolayers and interfacial water at the air-water interface. *Langmuir* **2015**, *31* (7), 2147-2156.
- 501 (9) Tervahattu, H.; Hartonen, K.; Kerminen, V. M.; Kupiainen, K.; Aarnio, P.; Koskentalo, T.; Tuck,
502 A. F.; Vaida, V. New evidence of an organic layer on marine aerosols. *J. Geophys. Res.: Atmos.* **2002**,
503 *107* (D7), 4053.

504 (10) Donaldson, D. J.; Vaida, V. The influence of organic films at the air-aqueous boundary on
505 atmospheric processes. *Chem. Rev.* **2006**, *106* (4), 1445-1461.

506 (11) Ellison, G. B.; Tuck, A. F.; Vaida, V. Atmospheric processing of organic aerosols. *J. Geophys.*
507 *Res.: Atmos.* **1999**, *104* (D9), 11633-11641.

508 (12) Feingold, G.; Chuang, P. Y. Analysis of the influence of film-forming compounds on droplet
509 growth: Implications for cloud microphysical processes and climate. *J. Atmos. Sci.* **2002**, *59* (12),
510 2006-2018.

511 (13) Vaida, V. Atmospheric radical chemistry revisited Sunlight may directly drive previously
512 unknown organic reactions at environmental surfaces. *Science* **2016**, *353* (6300), 650-650.

513 (14) Zhang, T.; Cathcart, M. G.; Vidalis, A. S.; Allen, H. C. Cation effects on phosphatidic acid
514 monolayers at various pH conditions. *Chem. Phys. Lipids* **2016**, *200*, 24-31.

515 (15) Li, S. Y.; Du, L.; Wei, Z. M.; Wang, W. X. Aqueous-phase aerosols on the air-water interface:
516 Response of fatty acid Langmuir monolayers to atmospheric inorganic ions. *Sci. Total Environ.* **2017**,
517 *580*, 1155-1161.

518 (16) Larsen, M. C. Binary phase diagrams at the air-water interface: An experiment for undergraduate
519 physical chemistry students. *J. Chem. Educ.* **2014**, *91* (4), 597-601.

520 (17) Adams, E. M.; Casper, C. B.; Allen, H. C. Effect of cation enrichment on
521 dipalmitoylphosphatidylcholine (DPPC) monolayers at the air-water interface. *J. Colloid Interface*
522 *Sci.* **2016**, *478*, 353-364.

523 (18) Rouviere, A.; Ammann, M. The effect of fatty acid surfactants on the uptake of ozone to aqueous
524 halogenide particles. *Atmos. Chem. Phys.* **2010**, *10* (23), 11489-11500.

525 (19) Shrestha, M.; Luo, M.; Li, Y.; Xiang, B.; Xiong, W.; Grassian, V. H. Let there be light: stability
526 of palmitic acid monolayers at the air/salt water interface in the presence and absence of simulated
527 solar light and a photosensitizer. *Chem. Sci.* **2018**, *9* (26), 5716-5723.

528 (20) Mochida, M.; Kitamori, Y.; Kawamura, K.; Nojiri, Y.; Suzuki, K. Fatty acids in the marine
529 atmosphere: Factors governing their concentrations and evaluation of organic films on sea-salt
530 particles. *J. Geophys. Res.: Atmos.* **2002**, *107* (D17), 4325.

531 (21) Sicre, M. A.; Marty, J. C.; Saliot, A. n-Alkanes, fatty acid esters, and fatty acid salts in size
532 fractionated aerosols collected over the Mediterranean Sea. *J. Geophys. Res.: Atmos.* **1990**, *95* (D4),
533 3649-3657.

534 (22) Cincinelli, A.; Stortini, A.; Perugini, M.; Checchini, L.; Lepri, L. Organic pollutants in sea-
535 surface microlayer and aerosol in the coastal environment of Leghorn—(Tyrrhenian Sea). *Mar. Chem.*
536 **2001**, *76* (1-2), 77-98.

537 (23) Ehrhardt, M.; Osterroht, C.; Petrick, G. Fatty-acid methyl esters dissolved in seawater and
538 associated with suspended particulate material. *Mar. Chem.* **1980**, *10* (1), 67-76.

539 (24) Mukherjee, S.; Datta, A. Langmuir-Blodgett deposition selects carboxylate headgroup
540 coordination. *Phys. Rev. E* **2011**, *84* (4), 041601.

541 (25) Tang, C. Y.; Huang, Z. S. A.; Allen, H. C. Binding of Mg²⁺ and Ca²⁺ to palmitic acid and
542 deprotonation of the COOH headgroup studied by vibrational sum frequency generation spectroscopy.
543 *J. Phys. Chem. B* **2010**, *114* (51), 17068-17076.

544 (26) Gericke, A.; Brauner, J. W.; Erukulla, R. K.; Bittman, R.; Mendelsohn, R. In-situ investigation
545 of partially deuterated fatty acid and phospholipid monolayers at the air-water interface by IR
546 reflection-absorption spectroscopy. *Thin Solid Films* **1996**, *284* (1-2), 428-431.

547 (27) Tang, C. Y.; Allen, H. C. Ionic binding of Na⁺ versus K⁺ to the carboxylic acid headgroup of
548 palmitic acid monolayers studied by vibrational sum frequency generation spectroscopy. *J. Phys.*
549 *Chem. A* **2009**, *113* (26), 7383-7393.

- 550 (28) Teer, E.; Knobler, C. M.; Lautz, C.; Wurlitzer, S.; Kildae, J.; Fischer, T. M. Optical
551 measurements of the phase diagrams of Langmuir monolayers of fatty acid, ester, and alcohol
552 mixtures by brewster-angle microscopy. *J. Chem. Phys.* **1997**, *106* (5), 1913-1920.
- 553 (29) Simon-Kutscher, J.; Gericke, A.; Huhnerfuss, H. Effect of bivalent Ba, Cu, Ni, and Zn cations
554 on the structure of octadecanoic acid monolayers at the air-water interface as determined by external
555 infrared reflection-absorption spectroscopy. *Langmuir* **1996**, *12* (4), 1027-1034.
- 556 (30) Sinnamon, B. F.; Dluhy, R. A.; Barnes, G. T. Reflection-absorption FT-IR spectroscopy of
557 pentadecanoic acid at the air/water interface. *Colloids Surf., A* **1999**, *146* (1-3), 49-61.
- 558 (31) Nikolova, G. S.; Zhang, L.; Chen, X.; Chi, L.; Haufe, G. Selective synthesis and self-organization
559 at the air/water interface of long chain fluorinated unsaturated ethyl esters and alcohols. *Colloids Surf.,*
560 *A* **2008**, *317* (1-3), 414-420.
- 561 (32) Nieto-Suarez, M.; Vila-Romeu, N.; Prieto, I. Influence of different factors on the phase
562 transitions of non-ionic Langmuir monolayers. *Appl. Surf. Sci.* **2005**, *246* (4), 387-391.
- 563 (33) Nieto-Suarez, M.; Vila-Romeu, N.; Dynarowicz-Latka, P.; Prieto, I. The influence of inorganic
564 ions on the properties of nonionic Langmuir monolayers. *Colloids Surf., A* **2004**, *249* (1-3), 11-14.
- 565 (34) Pelletier, I.; Bourque, H.; Buffeteau, T.; Blaudez, D.; Desbat, B.; Pezolet, M. Study by infrared
566 spectroscopy of ultrathin films of behenic acid methyl ester on solid substrates and at the air/water
567 interface. *J. Phys. Chem. B* **2002**, *106* (8), 1968-1976.
- 568 (35) Gericke, A.; Hühnerfuss, H. The conformational order and headgroup structure of long-chain
569 alkanic acid ester monolayers at the air/water interface. *Ber. Bunsenges. Phys. Chem.* **1995**, *99* (4),
570 641-650.
- 571 (36) Gericke, A.; Huhnerfuss, H. In-situ investigation of saturated long-chain fatty-acids at the air-
572 water-interface by external infrared reflection-absorption spectrometry. *J. Phys. Chem.* **1993**, *97* (49),
573 12899-12908.
- 574 (37) Brzozowska, A. M.; Duits, M. H. G.; Mugele, F. Stability of stearic acid monolayers on artificial
575 sea water. *Colloids Surf., A* **2012**, *407*, 38-48.
- 576 (38) Kester, D. R.; Duedall, I. W.; Connors, D. N.; Pytkowicz, R. M. Preparation of artificial seawater.
577 *Limnol. Oceanogr.* **1967**, *12* (1), 176-179.
- 578 (39) Forestieri, S. D.; Staudt, S. M.; Kuborn, T. M.; Faber, K.; Ruehl, C. R.; Bertram, T. H.; Cappa,
579 C. D. Establishing the impact of model surfactants on cloud condensation nuclei activity of sea spray
580 aerosol mimics. *Atmos. Chem. Phys.* **2018**, *18* (15), 10985-11005.
- 581 (40) Khattari, Z.; Sayyed, M. I.; Qashou, S. I.; Fafous, I.; Al-Abdullah, T.; Maghrabi, M. Interfacial
582 behavior of myristic acid in mixtures with DMPC and cholesterol. *Chem. Phys.* **2017**, *490*, 106-114.
- 583 (41) Hao, C. C.; Sun, R. G.; Zhang, J. Mixed monolayers of DOPC and palmitic acid at the liquid-air
584 interface. *Colloids Surf., B* **2013**, *112*, 441-445.
- 585 (42) Griffith, E. C.; Guizado, T. R.; Pimentel, A. S.; Tyndall, G. S.; Vaida, V. Oxidized aromatic-
586 aliphatic mixed films at the air-aqueous solution interface. *J. Phys. Chem. C* **2013**, *117* (43), 22341-
587 22350.
- 588 (43) Minh Dinh, P.; Lee, J.; Shin, K. Collapsed States of Langmuir Monolayers. *J. Oleo Sci.* **2016**,
589 *65* (5), 385-397.
- 590 (44) Kaganer, V. M.; Mohwald, H.; Dutta, P. Structure and phase transitions in Langmuir monolayers.
591 *Rev. Mod. Phys.* **1999**, *71* (3), 779-819.
- 592 (45) Hasegawa, T.; Nishijo, J.; Watanabe, M.; Umemura, J.; Ma, Y. Q.; Sui, G. D.; Huo, Q.; Leblanc,
593 R. M. Characteristics of long-chain fatty acid monolayers studied by infrared external-reflection
594 spectroscopy. *Langmuir* **2002**, *18* (12), 4758-4764.
- 595 (46) Adams, E. M.; Allen, H. C. Palmitic acid on salt subphases and in mixed monolayers of
596 cerebrosides: Application to atmospheric aerosol chemistry. *Atmosphere* **2013**, *4* (4), 315-336.

597 (47) Nutting, G. C.; Harkins, W. D. Pressure-area relations of fatty acid and alcohol monolayers. *J.*
598 *Am. Chem. Soc.* **1939**, *61*, 1180-1187.

599 (48) Sierra-Hernandez, M. R.; Allen, H. C. Incorporation and exclusion of long chain alkyl halides in
600 fatty acid monolayers at the air-water interface. *Langmuir* **2010**, *26* (24), 18806-18816.

601 (49) Brzozowska, A.; Mugele, F.; Duits, M. Stability and interactions in mixed monolayers of fatty
602 acid derivatives on artificial sea water. *Colloids Surf., A* **2013**, *433*, 200-211.

603 (50) Yue, X. L.; Steffen, P.; Dobner, B.; Brezesinski, G.; Mohwald, H. Monolayers of mono- and
604 bipolar palmitic acid derivatives. *Colloids Surf., A* **2004**, *250* (1-3), 57-65.

605 (51) Gershevitz, O.; Sukenik, C. N. In situ FTIR-ATR analysis and titration of carboxylic acid-
606 terminated SAMs. *J. Am. Chem. Soc.* **2004**, *126* (2), 482-483.

607 (52) Johann, R.; Vollhardt, D. Texture features of long-chain fatty acid monolayers at high pH of the
608 aqueous subphase. *Mater. Sci. Eng., C* **1999**, *8*, 35-42.

609 (53) Wang, L.; Jacobi, S.; Sun, J.; Overs, M.; Fuchs, H.; Schaefer, H. J.; Zhang, X.; Shen, J.; Chi, L.
610 Anisotropic aggregation and phase transition in Langmuir monolayers of methyl/ethyl esters of 2, 3-
611 dihydroxy fatty acids. *J. Colloid Interface Sci.* **2005**, *285* (2), 814-820.

612 (54) Wang, Y.; Du, X.; Guo, L.; Liu, H. Chain orientation and headgroup structure in Langmuir
613 monolayers of stearic acid and metal stearate (Ag, Co, Zn, and Pb) studied by infrared reflection-
614 absorption spectroscopy. *J. Chem. Phys.* **2006**, *124* (13), 134706.

615 (55) Chen, Q. B.; Kang, X. L.; Li, R.; Du, X. Z.; Shang, Y. Z.; Liu, H. L.; Hu, Y. Structure of the
616 Complex Monolayer of Gemini Surfactant and DNA at the Air/Water Interface. *Langmuir* **2012**, *28*
617 (7), 3429-3438.

618 (56) Pelletier, I.; Laurin, I.; Buffeteau, T.; Desbat, B.; Pézolet, M. Infrared study of the molecular
619 orientation in ultrathin films of behenic acid methyl ester: comparison between single Langmuir-
620 Blodgett monolayers and spin-coated multilayers. *Langmuir* **2003**, *19* (4), 1189-1195.

621 (57) Muro, M.; Itoh, Y.; Hasegawa, T. A conformation and orientation model of the carboxylic group
622 of fatty acids dependent on chain length in a Langmuir monolayer film studied by polarization-
623 modulation infrared reflection absorption spectroscopy. *J. Phys. Chem. B* **2010**, *114* (35), 11496-
624 11501.

625 (58) Levin, I. W.; Thompson, T. E.; Barenholz, Y.; Huang, C. Two types of hydrocarbon chain
626 interdigitation in sphingomyelin bilayers. *Biochemistry* **1985**, *24* (22), 6282-6286.

627 (59) Aoki, P. H. B.; Morato, L. F. C.; Pavinatto, F. J.; Nobre, T. M.; Constantino, C. J. L.; Oliveira,
628 O. N., Jr. Molecular-Level Modifications Induced by Photo-Oxidation of Lipid Monolayers
629 Interacting with Erythrosin. *Langmuir* **2016**, *32* (15), 3766-3773.

630 (60) Huang, C. H.; Lapidés, J. R.; Levin, I. W. Phase-transition behavior of saturated, symmetric
631 chain phospholipid-bilayer dispersions determined by Raman-spectroscopy-correlation between
632 spectral and thermodynamic parameters. *J. Am. Chem. Soc.* **1982**, *104* (22), 5926-5930.

633 (61) Sakai, H.; Umemura, J. Molecular orientation in Langmuir films of 12-hydroxystearic acid
634 studied by infrared external-reflection spectroscopy. *Langmuir* **1998**, *14* (21), 6249-6255.

635 (62) Le Calvez, E.; Blaudez, D.; Buffeteau, T.; Desbat, B. Effect of cations on the dissociation of
636 arachidic acid monolayers on water studied by polarization-modulated infrared reflection-absorption
637 spectroscopy. *Langmuir* **2001**, *17* (3), 670-674.

638 (63) Avila, L.; Saraiva, S.; Oliveira, J. Stability and collapse of monolayers of stearic acid and the
639 effect of electrolytes in the subphase. *Colloids Surf., A* **1999**, *154* (1-2), 209-217.

640 (64) Griffith, E. C.; Adams, E. M.; Allen, H. C.; Vaida, V. Hydrophobic collapse of a stearic acid
641 film by adsorbed l-phenylalanine at the air-water interface. *J. Phys. Chem. B* **2012**, *116* (27), 7849-
642 7857.

643 (65) Gilman, J. B.; Tervahattu, H.; Vaida, V. Interfacial properties of mixed films of long-chain
644 organics at the air-water interface. *Atmos. Environ.* **2006**, *40* (34), 6606-6614.

- 645 (66) Gilman, J. B.; Eliason, T. L.; Fast, A.; Vaida, V. Selectivity and stability of organic films at the
646 air-aqueous interface. *J. Colloid Interface Sci.* **2004**, *280* (1), 234-243.
- 647 (67) Tervahattu, H.; Juhanoja, J.; Kupiainen, K. Identification of an organic coating on marine aerosol
648 particles by TOF-SIMS. *J. Geophys. Res.: Atmos.* **2002**, *107* (D16), 4319.
- 649 (68) Noziere, B.; Baduel, C.; Jaffrezo, J.-L. The dynamic surface tension of atmospheric aerosol
650 surfactants reveals new aspects of cloud activation. *Nat. Commun.* **2014**, *5*, 3335.
- 651 (69) Farmer, D. K.; Cappa, C. D.; Kreidenweis, S. M. Atmospheric Processes and Their Controlling
652 Influence on Cloud Condensation Nuclei Activity. *Chem. Rev.* **2015**, *115* (10), 4199-4217.
- 653 (70) Gorbunov, B.; Hamilton, R.; Clegg, N.; Toumi, R. Water nucleation on aerosol particles
654 containing both organic and soluble inorganic substances. *Atmos. Res.* **1998**, *48*, 271-283.

655